*Int. J. Electrochem. Sci.*, 17 **(2022)** Article Number: 221276, doi: 10.20964/2022.12.89

International Journal of
ELECTROCHEMICAL
SCIENCE
www.electrochemsci.org

# In Situ Growth of $Co(OH)_2$/NiS on Cobalt Foam for Supercapacitor Application

*Zhe Li*[1,2], *Chun-yong Zhang*[1,2,*], *Hao-yu Wang*[1], *Lin Zhu*[1], *Hai-tao Liu*[1], *Li Shu*[2], *Ying-pin Weng*[2]

[1] School of Chemistry and Environmental Engineering, Jiangsu University of Technology, Changzhou, 213001, China
[2] Jiangsu Key Laboratory of Precious Metal Chemistry and Technology, Jiangsu University of Technology, Changzhou, 213001, China
[*] E-mail: zhangcy@jsut.edu.cn

*Received:* 17 October 2022 / *Accepted:* 28 November 2022 / *Published:* 27 December 2022

---

Herein, a simple hydrothermal method was used to synthesize cobalt hydroxide/nickel sulfide and cobalt foam ($Co(OH)_2$/NiS@CF) composite electrode. By simply heating cobalt foam in the aqueous solution containing cobalt nitrate, nickel nitrate, and thiourea, $Co(OH)_2$/NiS nano stereoscopic website was synthesized on Cobalt foam. X-Ray Diffraction (XRD), Scanning Electron Microscopy (SEM), and electrochemical tests were used to characterize these composite electrodes. When the molar ratio of $Co(NO_3)_2{\cdot}6H_2O$ to Thiourea of 4:5, $Co(OH)_2$/NiS@CF exhibits excellent performance under these tests. The specific capacitance was 1260 F/g at 1.0 A/g. The composite electrode had 92.3% capacitance retention after 2000 charge-discharge cycles at 1.0 A/g.

---

**Keywords:** Cobalt foams (CF); $Co(OH)_2$; Sulfuration; Composite materials; Electro-chemical properties

## 1. INTRODUCTION

With the rise of the global economy and population, energy issues have gotten attention from researchers. The development of clean energy (solar energy, tidal energy, wind energy, etc.) has alleviated the energy crisis and environmental problems[1-3]. However, these energies usually need mechanical energy or photothermoelectric effect to convert into electricity, and the conversion efficiency is low[4-6]. Electrochemical energy conversion/storage devices have attracted extensive attention in the past several decades. For example, supercapacitors manifest outstanding power density, high-efficiency charge and discharge performance, long cycle life, and large capacity[7-10]. The energy storage of supercapacitors is limited by electrode material. The key factors that affect the electrode material are morphology, porosity, and specific surface areas. Of late years, many scholars dedicate to the study electrochemical performance of porosity[11-13]. Transition metal hydroxides with high specific capacity, low cost, and environmental friendliness also have the potential to be an electrode material for supercapacitors[14].

In recent years, many researchers have designed electrochemical energy storage with morphology and material composition on three-dimensional (3D) conductive current collectors (Ni foam or Cu foam) to improve energy storage performance[15-18]. Metal foams have three-dimensional frameworks with good mechanical strength, excellent electrical conductivity, and porous morphology, providing large surface area and multidimensional electron transport pathways. This property can avoid the blocking of active sites and reduce the overload caused by ionic resistance and charge transfer[19,20]. At the same time, the porous channel and high specific surface area are beneficial to improve the activity of materials, so these characteristics make the metal foams more suitable for supporting the catalytic active material than the metal body itself[21]. Many previous studies have used commercial nickel foam, but the poor pore structure, low porosity, and large pore size (450 - 3200 μm) restrict its development. This results in a large gap between actual and expected performance[22].

In previous reports, the metal foam has been used to research electrocatalysis. For example, Zhang et al. embedded petal-shaped $Co_3O_4$ composed of microstrips in the large pores of the cobalt foam through the hydrothermal process and calcination process, and finally, $Co_3O_4$@Co foam showed high oxygen evolution activity[23]. The direct contact between $Co_3O_4$ microstrip and cobalt foam greatly increased the surface area of the reaction and improved the catalytic activity of the composite. Among the known studies, there is litter literature about the application of cobalt foam in electrode materials, and there is also a large space for development in improving the performance of electrode materials. Dai et al. synthesized Co foam@$Co_3O_4$ porous nanosheet arrays by in situ oxidation reaction[24]. The nanosheets with a thickness of 3 nm were filled with micropores with a diameter of about 5 nm. The prepared Co foam@$Co_3O_4$ material had high specific capacitance but very small resistance. It also showed significant long-term stability, maintaining 77.5% permittivity after 20,000 charges.

Fu et al. fabricated a self-supporting electrode (cobalt foam) by in situ growth of $Co_3O_4$($Co_3O_4$/CF)[25]. The contact between the needle-like Owing to the needle-like $Co_3O_4$ and cobalt foam caused the working electrode's electrochemical performance to improve on charge-transport properties and electrocatalytic activity. Zhao et al. used a one-step hydrothermal method to in situ grow an urchin-like ternary nanocomposite (NRC) on cobalt foam[26]. As-synthesized NRC@Co foam had a hierarchically porous structure, which delivered excellent electrochemical performances. The specific capacitance at a current density of 0.56 A/g was 10237.5 F/g, and the permittivity was maintained at 117.8% after 14,000 charges and discharges.

According to the above references, we used cobalt foam as a self-support material and loaded metal materials on its surface because of its extensive specific surface area. As shown in Fig. 1, the cobalt foam (CF) was pretreated firstly, and then the Co-Ni bimetallic precursor was obtained by the hydrothermal method, which was then calcined in a tube furnace and then subjected to hydrothermal treatment to complete the sulfuration. Finally, $Co(OH)_2$ was synthesized in the $Co(OH)_2$/NiS@CF composite and tested its electrochemical performance in an alkaline electrolyte. The effect of sulfurization degree on the microstructure and electrochemical properties of $Co(OH)_2$/NiS@CF was investigated.

## 2. EXPERIMENTAL

### *2.1. Materials*

All reagents in experiments were of analytical level and used without further treatment. Cobalt Nitrate Hexahydrate, Nickel Nitrate Hexahydrate, Urea, and Thiourea were supplied by Shanghai Aladdin Biochemical Technology Co., Ltd. Ammonium fluoride and Ethanol were supplied by Sinopharm Group Chemical Reagent Shanghai Co., Ltd. Cobalt foam was supplied by Kunshan Guangjia New Material Co., Ltd. Acetone was supplied by Shanghai Lingfeng Chemical Reagent Co., Ltd. Deionized water was used throughout the study.

### *2.2. Pretreatment of CF*

The cobalt foam collectors (CF, 1 cm × 2 cm) were carefully washed with 3.0 M HCl for 30 min and then washed respectively with acetone (BLE), ethanol (EtOH), and deionized water (DIW) for 10 min to remove surface impurities. Afterward, CF was dried in the oven.

### *2.3. Preparation of $Co(OH)_2/NIS_x$@CF material*

Firstly, 0.58 g $Co(NO_3)_2{\cdot}6H_2O$, 0.29 g $Ni(NO_3)_2{\cdot}6H_2O$, 0.6 g $CO(NH_2)_2$ and 0.6 g $NH_4F$ were added to 40 mL DIW. The mixture was stirred at room temperature until well mixed to ensure that both sides were in full contact with the solution, and then the mixed system was moved to a 50 mL Teflon-lined stainless steel autoclave. The as-prepared CF was immersed into the Teflon-lined stainless steel autoclave and kept at 100 ºC for 6 h. After completion of the reaction, the temperature was cooled to room temperature. CF was removed from the Teflon-lined stainless steel autoclave and washed with DIW and EtOH to remove impurities. And then the CF dried in an oven at 60 ºC for 12 h. Furthermore, the as-prepared CF was placed in a tube and then heated at 350 ºC for 2h at the heating rate of 5 ºC/min under flowing $N_2$ gas.

The amount of Thiourea was added to 35 mL DIW, under constant mechanical stirring to obtain a transparent solution. CF prepared above was immersed in a transparent solution slowly to ensure that it can sufficiently contact with the solution. And then CF was poured into a Teflon-lined stainless steel autoclave for hydrothermal reaction. The obtained precipitate was thoroughly washed three times with EtOH and DIW respectively. Placing it in an oven to dry completely and setting aside. Among them, Thiourea is a sulfur source, and the molar mass ratio of cobalt source to thiourea was respectively 4:3, 4:4, and 4:5. According to different ratios, the corresponding composites were denoted as $Co(OH)_2/NiS_x$@CF (x=3, 4, 5).

Fig. 1 shows the fabrication process of the $Co(OH)_2/NiS_x$@CF.

### *2.4. Material characterization*

X-Ray Diffraction (XRD) of all as-synthesized samples was collected on SmartLab 9 kw. Scanning electron microscope (SEM) images and Energy Dispersive X-ray (EDX) were obtained from

Zeiss Sigma 300.

### *2.5. Electrochemical measurements*

All electrochemical characterization and performance were tested by an electrochemical workstation (CHI760E, China) using a standard three-electrode at room temperature. The cyclic voltammetry (CV), the galvanostatic charge-discharge (GCD), and the electrochemical impedance spectrum (EIS) were performed in 6.0 M KOH. The $Co(OH)_2/NiS_x@CF$, a Pt sheet, and saturated a calomel electrode (Hg/HgO) were used as the working, counter, and reference electrodes respectively. The exposure area on the working electrode for electrochemical testing was approximately about 1 cm × 1 cm. CV was tested by starting cycling between 0.15 and 0.3 V at scan rates within 5 - 80 mV/s. GCD was tested in a potential window between 0.15 and 0.3 V at different current densities within 1.0-5.0 A/g. EIS was conducted in the range from 0.01 - 100000Hz with an alternating amplitude of 5 mV. The specific capacitance ($C_s$) values of $Co(OH)_2/NiS_x@CF$ is estimated using equation (1):

$$C_s = (I \times \Delta t)/(m \times \Delta V) \qquad (1)$$

Where $Cs$ (F/g) is the specific capacitance, $I$ (A) is the discharge current, $m$ (g) is the weight of material on the working electrode area, $\Delta t$ (S) is the discharge time, and $\Delta V$ (V) is the potential window.

**Figure 1.** Synthesis scheme of $Co(OH)_2/NiS_x@CF$ composites.

## 3. RESULTS AND DISCUSSION

Fig. 2 shows XRD patterns of $Co(OH)_2/NiS_x@CF$. The XRD patterns of the three materials have the same characteristic peak positions with different peak intensities. For CF, the diffraction peaks at 41.7°, 44.7°, 47.6°, and 62.7° could correspond to the (100), (002), (101), and (110) planes of Co (JSPDS 05-0727). The obvious diffraction peaks at 19.1°, 32.6°, 38.0°, 51.5°, and 59.7° could correspond to the (001), (100), (011), (012), and (003) planes of $Co(OH)_2$ (JSPDS 74-1054) after cobalt foam and metal salt complete hydrothermal reaction and sulfuration. The peaks of NiS appear at 18.4°, 32.2°, 37.3°, 50.1°, and 59.7° could correspond to the (100), (300), (220), (410), and (012) planes. $Co(OH)_2/NiS_x@CF$ was successfully obtained from the analysis of XRD. $Co(OH)_2/NiS@CF$ has strong crystallization peaks when the molar mass ratio cobalt source to thiourea is respectively 4:5.

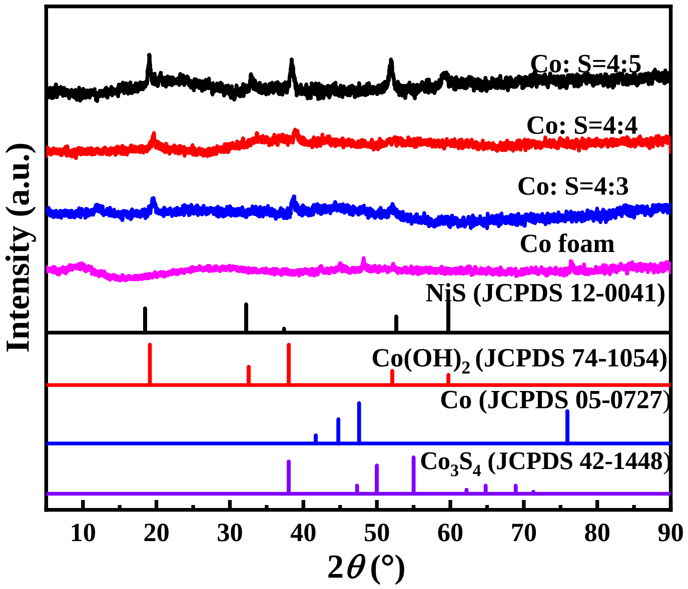

**Figure 2.** XRD patterns of CF and $Co(OH)_2/NiS_x$@CF.

The morphologies of the $Co(OH)_2/NiS_x$@CF were characterized by SEM. As shown in Fig. 3a, it is observed that the microstructure of cobalt foam exhibits a three-dimensional skeleton structure and metal compounds are easy to be loaded because of their rough surface. From Fig. 3b, the microstructure of $Co(OH)_2/NiS_5$@CF exhibits interconnected nanosheets and forms a three-dimensional network under hydrothermal reaction. This three-dimensional network not only avoids cluttered stacking in space but also increases the specific surface area. The increase of specific surface area leads to more active removal of active sites in contact with the electrolyte, which improves the electrochemical performance. At the same time, as a current collector with good electrical conductivity, cobalt foam can enhance the ability of charge transfer. The SEM image in Fig. 3c reveals that the microstructure of $Co(OH)_2/NiS_4$@CF exhibits urchin-like microspheres. Urchin-like microspheres can add more catalytically active sites. From Fig. 3d, the microstructure of $Co(OH)_2/NiS_3$@CF exhibits a nanoarray shape and was crimped into a three-dimensional structure.

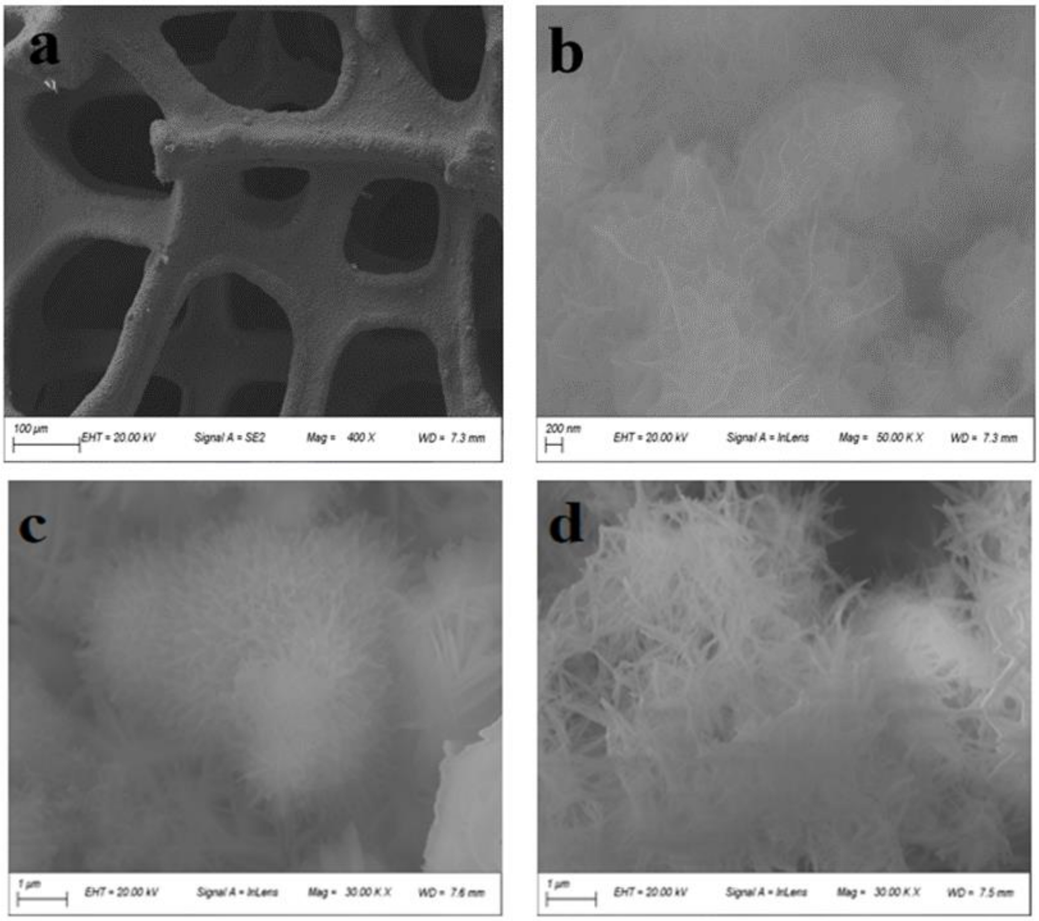

**Figure 3.** SEM images of CF (a), $Co(OH)_2/NiS_5@CF$ (b) $Co(OH)_2/NiS_4@CF$ (c), and $Co(OH)_2/NiS_3@CF$ (d).

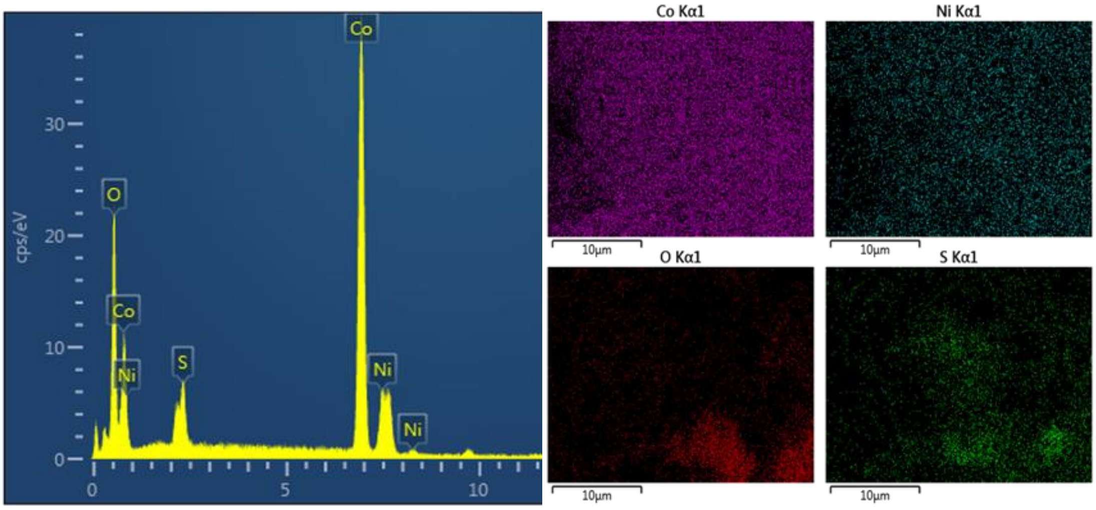

**Figure 4.** EDX and Elemental mapping of $Co(OH)_2/NiS_5@CF$.

The EDX analysis (Fig. 4) of $Co(OH)_2/NiS_5@CF$ reveals that the material contains Co, Ni, O, and S elements, confirming that $Co(OH)_2/NiS_5@CF$ was successfully synthesized. From Table 1, the atomic ratios of Co, Ni, O, and S are 60.0 %, 11.5 %, 22.6 %, and 5.9 %. Good sulfuration treatment can effectively improve the electron transfer rate.

**Table 1.** The element distribution in $Co(OH)_2/NiS_5$@CF.

| Element | Weight percent % | Atomic percent % |
|---|---|---|
| O | 9.7 | 22.6 |
| Co | 72.1 | 60.0 |
| Ni | 15.4 | 11.5 |
| S | 2.8 | 5.9 |

Fig. 5(a-c) shows the CV curves of $Co(OH)_2/NiS_x$@CF. The CV at all the scanning rates ranges from 5 to 80 mV/s. All CV curves of $Co(OH)_2/NiS_x$@CF show no oxidation reduction peak, which indicates the electrochemical stability and energy storage of the electrode material based on the double electric layer. Meanwhile, as the scanning rate is increased, the current also is increased, the phenomenon indicates that the electrode material has high ion transfer and high-rate electrochemical properties. All CV curves show the characteristics of double-layer capacitance, the rectangular-like shape refers to the accumulation of capacitance by electrolyte ions at the interface between electrode and electrolyte. In addition, even if on a high scanning rate, the shape of CV curves can be kept unaltered. This proves that these materials have high-rate electrochemical properties[27]. On the other hand, the CV curves of $Co(OH)_2/NiS_5$@CF material has the largest area at the same scanning rate, which indicates that the material has the best electrochemical performance under these conditions of sulfuration.

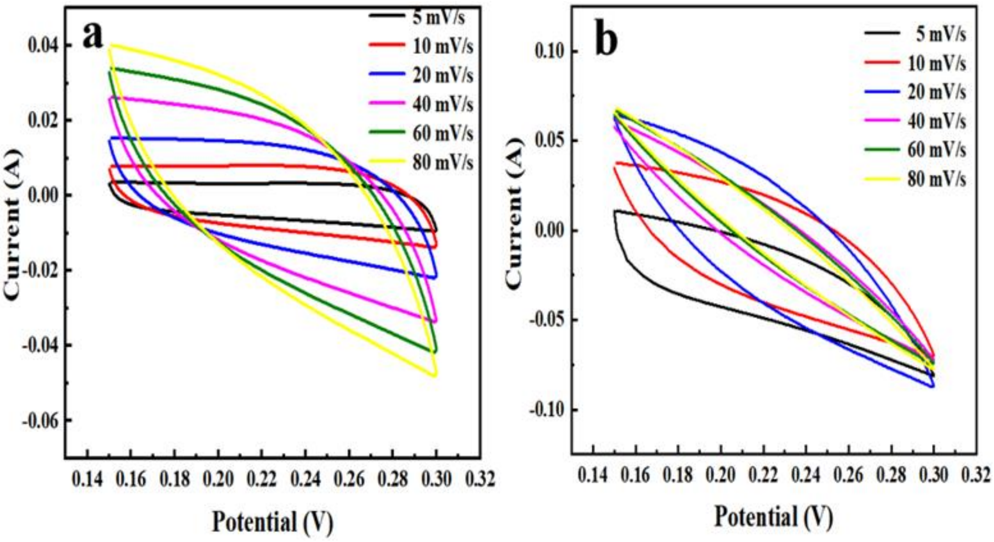

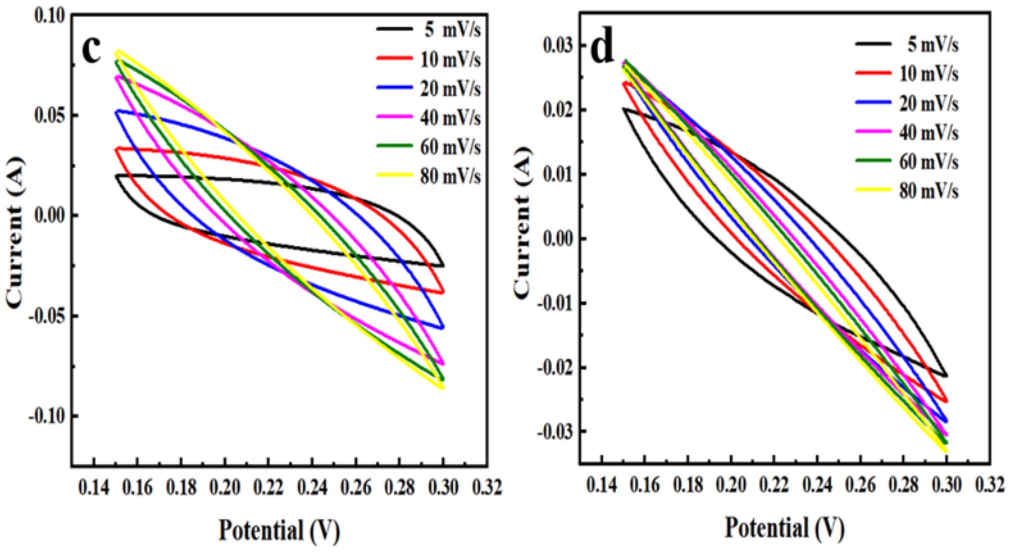

**Figure 5.** The CV of Co(OH)$_2$/NiS$_3$@CF (a) Co(OH)$_2$/NiS$_4$@CF (b) Co(OH)$_2$/NiS$_5$@CF (c), and CF (d).

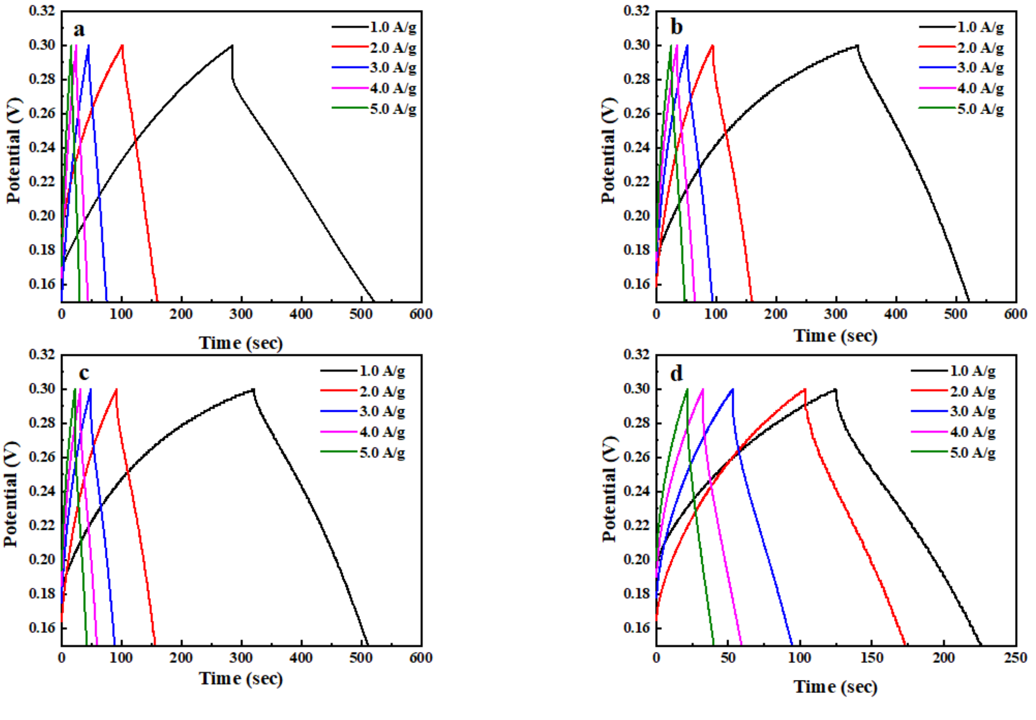

**Figure 6.** GCD curves of Co(OH)$_2$/NiS$_5$@CF (a) Co(OH)$_2$/NiS$_4$@CF (b) Co(OH)$_2$/NiS$_3$@CF (c), and CF (d).

The GCD curves of CF and Co(OH)$_2$/NiS$_x$@CF at current densities within 1.0-5.0 A/g are shown in Fig. 6. It can be observed that the resulting material after sulfuration takes longer to charge and discharge than the original. Electrochemical properties can be improved under the action of sulfuration. When Co:S is 4:5, the corresponding material has the longest charging time. Fig. 7a shows the specific capacitance of four electrodes at 1.0 A/g. The specific capacitance of CF is 669 F/g, while the specific capacitances of $Co(OH)_2/NiS_x@CF$ (x=3, 4, 5) are 1100 F/g, 1160 F/g, and 1260 F/g. At the same current density, the specific capacitance of $Co(OH)_2/NiS_5@CF$ is the biggest. That's probably because the 3D network structure not only increases the specific surface area and ion transport capacity but also increases the available active sites. The following chemical reactions show the oxidation reaction: [28,29]

$Co(OH)_2 + OH^- \leftrightarrow CoOOH + H_2O + e^-$ (2)

$CoOOH + OH^- \leftrightarrow CoO_2 + H_2O + e^-$ (3)

$NiS + OH^- \leftrightarrow NiSOH + e^-$ (4)

$NiSOH + OH^- \leftrightarrow NiSO + H_2O + e^-$ (5)

The EIS of the $Co(OH)_2/NiS_x@CF$ is shown in Fig. 7b. CF alone has no semicircle, indicating low charge transfer resistance on the electrode surface. $Co(OH)_2/NiS_x@CF$ with different degrees of sulfuration have semicircles of varying sizes.

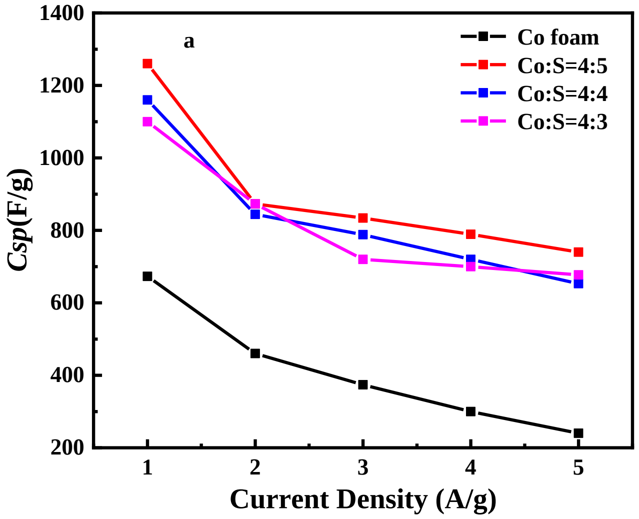

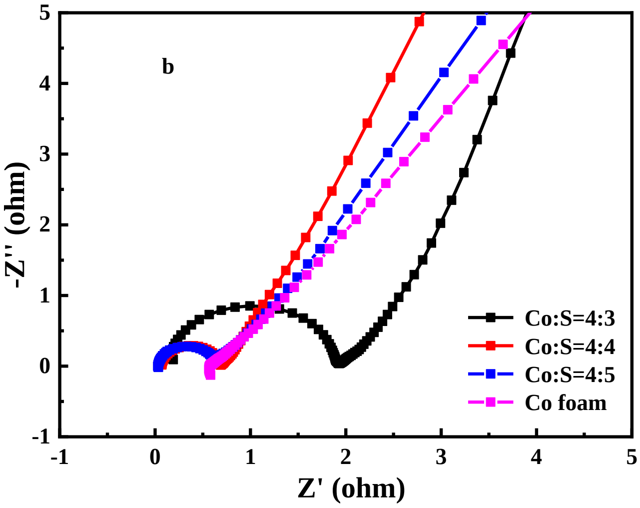

**Figure 7.** The specific capacitance (a) and the EIS (b) of CF and different ratios of $Co(OH)_2/NiS_x@CF$.

The resistances of $Co(OH)_2/NiS_x@CF$ (x=3, 4, 5) were 0.63 Ω, 0.15 Ω, and 0.10 Ω by calculating the sizes of the semicircle. According to the data, the obtained $Co(OH)_2/NiS_x@CF$ composite electrode material has better electrocatalytic activity than pure CF. The reason may be that in situ growth of $Co(OH)_2/NiS$ on the cobalt foam reduces the resistance of the electrode and facilitates the interfacial electron transfer.

Fig. 8 shows the cyclic stability of CF and $Co(OH)_2/NiS_x@CF$ at 1.0 A/g, it can be observed that $Co(OH)_2/NiS_x@CF$ which grows directly and vulcanized on the surface of cobalt foam improves significantly cycle performance, the composite material has stronger cycling performance than pure CF. Especially $Co(OH)_2/NiS_5@CF$ shows the most excellent performance, after 2000 charge-discharge cycles, the remained specific capacitance is 93.2%. We believe the excellent cycling performance of $Co(OH)_2/NiS_5@CF$ is due to $Co(OH)_2/NiS$ with a 3D network structure.

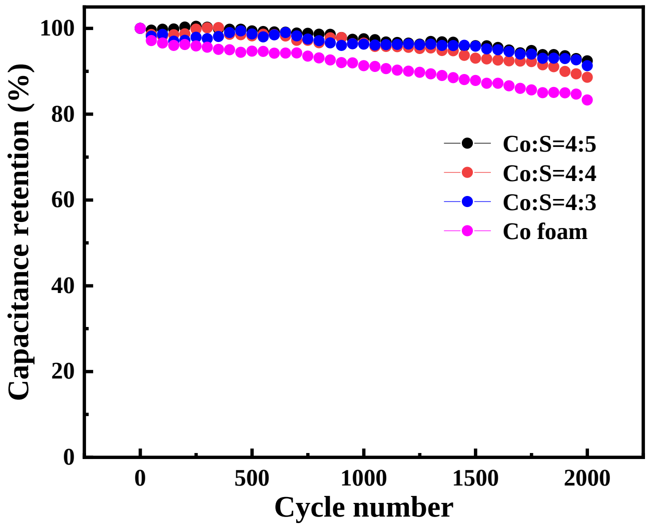

**Figure 8.** Cyclic stability of CF and $Co(OH)_2/NiS_x@CF$ at 1.0 A/g.

**Table 2.** Comparison of the electrochemical property of the $Co(OH)_2/NiS_5@CF$ composite in this work with previously reported materials.

| Electrode Material | Test Solution | Specific capacitance (F/g) | Current density (A/g) | Reference |
|---|---|---|---|---|
| $Co(OH)_2$ | 1.0 M KOH | 756 | 4.0 | [30] |
| $Ni-Co(OH)_2$ | 1.0 M KOH | 1664 | 5.0 | [31] |
| $NiCo_2S_4@PPy/NF$ | 3.0 M KOH | 2554.9 | 2.54 | [32] |
| Ni/Co LDH | 6.0 M KOH | 1575 | 1.0 | [33] |
| $Co(OH)_2/NiS_5@CF$ | 6.0 M KOH | 1260 | 1.0 | This work |

## 4. CONCLUSIONS

In summary, $Co(OH)_2/NiS_5@CF$ with a 3D network structure was successfully fabricated by a two-step hydrothermal method. The prepared $Co(OH)_2/NiS_5@CF$ electrode for its electrochemical and structural properties had good performances. The material's structural properties revealed the successful synthesis of 3D net-work material that eventually could deliver the energy storing purpose perfectly. The 3D network of $Co(OH)_2/NiS_5@CF$ provided more electroactive sites and a pathway for electron transfer and electrolyte diffusion. This resulted in the remarkable specific capacitance of 1260 F/g at a current density of 1.0 A/g, and the resistance was only 0.10 Ω. The sample also showed excellent stability of 93.2% capacitance retention over 2000 charge-discharge cycles at 1.0 A/g. In addition to the wide composite material, $Co(OH)_2/NiS_5@CF$ in this study may be accounted as a new scheme in the field of supercapacitors.

DECLARATION OF COMPETING INTEREST
The authors declare that we have no conflicts of interest.

ACKNOWLEDGEMENTS
This work was financially supported by Postgraduate Research & Practice Innovation Program of Jiangsu Province (SJCX22_1456) and (SJCX22_1459), Innovation and Entrepreneurship Training program for College students in Jiangsu Province (Haitao Liu), National Natural Science Foundation of China (grant no. 31800495), Natural Science Foundation of Jiangsu Province (grant no. BK20181040).

## References

1. J. B. Qin, X. Y. Chi, J. J. You, C. Q. Du and S. Q. Cheng. *Int J Electrochem Sci.*, 17 (2022) 220335.
2. A. Manalu, K. Tarigan, S. Humaidi, M. Ginting, K. Sebayang, M. Rianna, M. Hamid, A. Subhan, P. Sebayang and I. P. Manalu. *Int J Electrochem Sci.,* 17 (2022) 22036.
3. L. L. Liu, M. Y. Li, Y. H. Sun, M. X. Ma, X. Y. Yang and H. Wang. *Int J Electrochem Sci.,* 17 (2022) 22031.
4. C. X. Miao, C. L. Zhou, H. E. Wang, K. Zhu, K. Ye, Q. Wang, J. Yan, D. X. Cao, N. Li and G. L. Wang. *J Power Sources.*, 490 (2021) 229532.
5. A. Muhammad, M. Tahir, S. S. Al-Shahrani, A. M. Ali and S. U. Rather. *Appl Surf Sci.*, 504 (2020) 144177.
6. J. Ren, M. Shen, Z. L. Li, C. M. Yang, Y. Lang, H. E. Wang, J. H. Li, N. Li and D. Qian. *J Power Sources.*, 501 (2021) 230003.
7. J. N. Li, C. Y. Zhang, Y. P. Wen, Y. Y. Zhao. Y. W. Zhang, L. Shu and H. F. Qin. *J Chem Res.*, 45 (2021) 983.
8. Y. H. Zhou, X. Ren, M. Y. Song, Y. Y. Du, J. F. Wan, G. Wu and F. W. Ma. *Renew Energy.*, 153 (2020) 1005.
9. E. Vivek, A. Arulraj, M. Khalid and I. V. Potheher. *J Alloys Compd.*, 908 (2022) 164541.
10. X. Y. Kang, J. W. Wang, Y. X. Ma, X. F. Shi, X. Q. Chen, H. Tian and F. Ran. *J Solid State Chem.*, 310 (2022) 123056.
11. Y. Yu, A. Xu, Y. Zhang, W. Li and Y. J. Qin. *Chem Eng J.*, 445 (2022) 136727.
12. S. K. Li, R. Wang, M. Xie, Y. C. Xu, J. R. Chen and Y. Jiao. *J Colloid Interface Sci.*, 622 (2022)

378.

13. Y. N. Guo, C. Hao, X. K. Wang, Y. Yang, X. H. Wang, J. B. Wu and Y. T. Shen. *Ceram Int.*, 48 (2022) 17644.
14. S. Bai, C. M. Wang, M. S. Deng, M. Gong, Y. Bai, J. Jiang and Y. J. Xiong. *Angew Chem Int Ed Engl.*, 53 (2014) 12120.
15. Z. Q. Wu, H. Li, H. Li, B. B. Yang, R. H. Wei, X. G. Zhu, X. B. Zhu and Y. P. Sun. *Chem Eng J.*, 444 (2022) 136597.
16. Z. Q. Wu, B. B. Yang, H. Li, H. Y. Tong, X. Wang, C. D. Li, L. L. Zhu, R. H. Wei, L. Hu, C. H. Liang, X. B. Zhu and Y. P. Sun. *J Power Sources.*, 507 (2021) 230269.
17. J. Liu, L. X. Ren, J. J. Luo and J. Song. *Colloids Surf A Physicochem Eng Asp.*, 647 (2022) 129093.
18. N. X. Zhang, T. Zhao, L. Wei, T. Feng, F. Wu and R.J. Chen. *J Power Sources.*, 536 (2022) 231374.
19. Y. J. Fu, C. Zhu, C. G. Liu, M. L. Zhang, H. B. Wang, W. L. Shi, H. Huang, Y. Liu and Z. H. Kang. *Appl Catal B.*, 226 (2018) 295.
20. J. Zhang, Q. Y. Zhang and X. L. Feng. *Adv Mater.*, 31 (2019) e1808167.
21. Y. J. Yang, M. X. Liu, C. J. Jiang, P. X. Yang, N. Y. Wang, S. Y. Chen and Y. Cheng. *J Energy Storage.*, 44 (2021) 103462.
22. H. X. Jia, S. Lu, S. H. Shin, M. L. Sushko, X. P. Tao, M. Hummel, P. Thallapally, J. Liu and Z. R. Gu. *J Power Sources.*, 526 (2022) 231163.
23. L. Zhang, Q. M. Liang, P. Yang, Y. Huang, W. J. Chen, X. M. Deng, H. H. Yang, J. H. Yan and Y. N. Liu. *Int J Hydrogen Energy.*, 44 (2019) 24209.
24. Y. M. Dai, S. S. Zhu, C. C. Wang, Y. Cong, Y. H. Zeng, T. T. Jiang, H. H. Huang, S. H. Huang and X. K. Meng. *J Alloys Compd.*, 748 (2018) 291.
25. J. Fu, F. B. Yao, T. Xie, Y. Zhong, Z. T. Tao, S. J. Chen, L. He, Z. J. Pi, K. J. Hou, D. B. Wang, X. M. Li and Q. Yang. *Sep Purif Technol.*, 276 (2021) 119329.
26. C. J. Zhao, S. Q. Wang, Z. Q. Zhu, P. W. Ju, C. H. Zhao and X. Z. Qian. *J Mater Chem A Mater.*, 5 (2017) 18594.
27. E. Cevik, S. T. Gunday, I. Anil, O. Alagha and A. Bozkurt. *Int J Energy Res.*, 44 (2020) 3203.
28. K. Song, W. T. Li, R. Yang, Y. J. Zheng, X. S. Chen, X. Wang, G. L. Chen and W. C. Lv. *Electrochim Acta.*, 388 (2021) 138663.
29. W. Wu, P. Xia, Y. W. Xuan, R. Yang, M. Chen and D. L. Jiang. *Nanotechnology.*, 31 (2020) 405705.
30. T. Deng, W. Zhang, O. Arcelus, J. G. Kim, J. Carrasco, S. J. Yoo, W. T. Zheng, J. F. Wang, H. W. Tian, H. B. Zhang, X. Q. Cui and T. F. Rojo. *Nat Commun.,* 1 (2017) 15194.
31. H. Deng, T. Liu, W. P. Liao and D. Z. Yang. *J Phys Chem Solids*., 164 (2022) 110641.
32. M. Barazandeh, S. H. Kazemi. *Sci Rep.,*12 (2022) 4628.
33. Z. Liu, H. T. Zhou. F. Zeng, L. H. Hu, X. Y. Song, C. Z. Jiang and X. G. Zhang. *ACS Appl Energy Mater.,* 5 (2022) 9418.